Compatibilization Efficiency of Styrene–Butadiene Triblock Copolymers in Polystyrene–Polypropylene Blends with Varying Compositions

D. Hlavatá,[1] J. Hromádková,[1] I. Fortelný,[1] V. Hašová,[1] J. Pulda[2]

[1]*Institute of Macromolecular Chemistry, Academy of Sciences of the Czech Republic, Heyrovsky Square 2, 162 06 Prague 6, Czech Republic*
[2]*Kaučuk Company, 278 52 Kralupy, Czech Republic*

Received 12 June 2003; accepted 4 November 2003

ABSTRACT: The compatibilization efficiency of two styrene-butadiene-styrene triblock copolymers with short (SB1) and long (SB2) styrene blocks was studied in polystyrene (PS)–polypropylene (PP) blends of composition 20, 50, and 80 wt % PS. The supramolecular structure of the blends was determined by small-angle X-ray scattering, and the morphology was studied with transmission electron microscopy and scanning electron microscopy. Structural changes in both the uncompatibilized and compatibilized blends were correlated with the values of tensile impact strength of these blends. Even though the compatibilization mechanisms were different in blends with SB1 and SB2, the addition of the block copolymers to the PS–PP 4/1 and PS–PP 1/4 blends led to similar structures and improved the mechanical properties in the same way. These block copolymers had a very slight effect on the impact strength in PS–PP 1/1 blends, exhibiting a nearly cocontinuous phase morphology. The strong migration of SB2 copolymers to the interface and of SB1 copolymers away from the interface were detected during the annealing of compatibilized PS–PP 4/1 blends. © 2004 Wiley Periodicals, Inc. J Appl Polym Sci 92: 2431–2441, 2004

Key words: blends; compatibilization; block copolymers; electron microscopy; SAXS

INTRODUCTION

It is generally known that most polymers are thermodynamically immiscible, and the modification of polymer blends by interfacially active compatibilizers is necessary to obtain materials with desirable properties. In polystyrene (PS)–polyolefin blends, additive compatibilization, that is, mixture with appropriate block copolymers (BCs), appears to be the most effective procedure,[1–23] although reactive compatibilization is now widespread. The addition of BCs with blocks miscible or at least compatible with the corresponding blend components reduces the interfacial tension between the constituent homopolymers and, thus, leads to their finer dispersion. Simultaneously, it increases the interfacial adhesion of the two phases.

The compatibilization efficiency of a BC is given by many parameters, including the number of blocks, the molecular weight (MW) of the individual blocks, its total MW, and of course, its chemical composition with respect to the blend components. In previous studies,[20–23] we investigated the compatibilization process in PS–polypropylene (PP) 4/1 blends, that is, in blends with a PS matrix with a series of BCs containing PS blocks and blocks of aliphatic hydrocarbons different from PP. The reason we used this procedure was that the synthesis of PS–PP BCs is rather expensive and another commercially available compatibilizer could be more convenient.

Considering our experimental data[20–23] and also the results of other studies,[5,8,9,11,13,16,17] we introduced the concept of symmetrical and asymmetrical systems.[24] In symmetrical systems (A–B blend and A–B BCs), good compatibilizers are BCs in which the MW of individual blocks is comparable with the MW of the corresponding homopolymers in a blend. In asymmetrical systems (A–B and A–B′; B is only chemically similar to B′), the copolymers, with A blocks long enough to form entanglements with the A homopolymer, are partially entrapped in this component of the blends, and they cannot easily take part in the formation of the A–B interfacial layer.

However, this phenomenon concerning the compatibilization in asymmetrical systems was observed in blends with the A matrix, and the results of some authors were contradictory to our conclusions. Radonjič and Musil[14] found a diblock copolymer, polystyrene-*block*-poly(ethene-*co*-propene), to be a relatively good compatibilizer for blends with PS–PP weight ratios of 10:90 and 30:70, even though the MW of its PS

Correspondence to: I. Fortelný (fortelny@imc.cas.cz).
Contract grant sponsor: Grant Agency of the Czech Republic; contract grant number: 106/02/1248.
Contract grant sponsor: Academy of Sciences of the Czech Republic; contract grant number: AVOZ 4050913.

TABLE I
Molecular Characteristics and Rheological Properties of the SB1 and SB2 Copolymers

Type	M_{theor}[a] (kg/mol)	M_p[b] (kg/mol)	M_n (kg/mol)	M_w (kg/mol)	PS_{theor}[c] (wt %)	PS_{GPC}[d] (wt %)	PS_{grav}[e] (wt %)	η^* (Pa s)	G' (Pa)
SB1	80	79	73	78	25.0	25.6	26.2	6.2×10^4	6.1×10^4
SB2	140	134	117	129	57.1	57.7	58.9	6.1×10^4	5.9×10^4

[a] M_{theor} = target molar mass.
[b] M_p = molar mass value for the most probable point on the SEC chromatograph.
[c] PS_{theor} = target molar mass concentration.
[d] PS_{GPC} = concentration of PS determined by GPC.
[e] PS_{grav} = concentration of PS determined by gravimetry after cleavage.

block (50,000) was remarkably higher than 18,000, that is, the critical MW necessary for entanglement formation.[25,26] Similarly, Harrats et al.[18] referred to polystyrene-*block*-poly(styrene-*co*-butene)-*block*-polybutene tapered diblocks with MWs of 23,000, 19,000, and 28,000, respectively, as effective compatibilizers in PS–low-density polyethylene (LDPE) blends rich in polyethylene (PE; PS–LDPE = 20:80).

Fortelný et al.[19] examined the compatibilization efficiency of a commercial styrene–butadiene (SB) BC in high-density PE and LDPE–high-impact PS blends of various compositions. They observed that the localization and structure of the BC depended to a large extent on the blend composition.

Because it is clear that the compatibilization efficiency of a BC is determined not only by its molecular architecture and the miscibility of its blocks with corresponding blend components but also by the composition of the studied blend, we decided to examine this problem in detail.

Recently, we synthesized two sets of diblock, triblock, and pentablock copolymers consisting of PB (MW = 60,000) and PS (MW = 10,000 or 40,000; Table I). The MW of the PS blocks in the first set was significantly lower than the critical value necessary for entanglement formation (~18,000), and the MW of PS blocks in the other set of BCs was sufficiently higher than this value. We verified the compatibilization efficiency of these BCs in both asymmetrical (PS–PP 4/1 and PS–PE 4/1) and symmetrical (PS–PB 4/1) systems.[23,24,27,28] All of the experimental results agreed well with our assumptions on different compatibilization processes in symmetrical and asymmetrical systems. As the triblock copolymers appeared to be the most effective compatibilizers, regardless of the length of the styrene blocks, for this work, we chose triblock copolymers with short and long styrene blocks. We studied their compatibilization efficiency in PS–PP blends of compositions 80, 50, and 20 wt % PS to find out how the blend composition affected both the localization and the internal structure of the BC in the final PS–PP–BC blends. With small-angle X-ray scattering (SAXS), transmission electron microscopy (TEM), and scanning electron microscopy (SEM), the structure of the blends with an addition of 5 or 10% a BC were investigated with three types of samples: quenched, slowly cooled, and annealed. In quenched samples, the structure of the molten state was assumed to be frozen; the slowly cooled samples underwent standard cooling. The structure results were correlated with the measurement of the stress-transfer properties of the blends.

EXPERIMENTAL

Materials

PS Krasten 171 was purchased from Kaučuk Co. [Kralupy, Czech Republic; M_w = 295,100, number-average molecular weight (M_n) = 64,100], and PP Mosten 52 492 was obtained from Chemopetrol (Litvínov, Czech Republic; M_w = 330,000, M_n = 51,000).

SB1 and SB2 BCs, pilot-plant products of Kaučuk Co., were prepared by anionic polymerization in *tert*-butyl methyl ether (MTBE) at 50°C with 1,4-dilithiobut-2-ene in MTBE as an initiator.[28,29] The total MW and the PS contents in the copolymers were determined by size exclusion chromatography–gel permeation chromatography with a dual refractive index and ultraviolet detection.[30] Moreover, the PS content was determined gravimetrically after the cleavage of styrene blocks with di-*tert*-butyl peroxide and osmium tetroxide (Table I).

Rheological measurements

The rheological properties of the BCs were measured on a Rheometrics SYS 4 rotational rheometer with antislipping parallel plates (Piscataway, NJ). The oscillatory shear measurements were carried out at 10^{-2}–10^2 rad/s at 190°C. The linear viscoelasticity regions for all of the samples were determined; the experiments were performed at strains between 3 and 7%. The values of complex viscosity (η^*) and elastic modulus (G'), obtained at a frequency of 1 rad/s, are summarized in Table I.

TABLE II
a_ϵ (kJ/m^2) of PS–PP Blends Compatibilized with SB BCs

	PS/PP 4/1		PS/PP 1/1 slowly cooled	PS/PP 1/4 slowly cooled
	Slowly cooled	Annealed		
PS–PP	11.0	9.5	32.6	27.2
+5% SB1	25.3		40.1	42.0
+10% SB1	29.0	20.6	41.5	43.6
+5% SB2	27.5		54.2	37.9
+10% SB2	30.0	44.9	55.0	58.2

Blend preparation

We prepared blends by mixing the components in the W 50 EH chamber of a Brabender plasticorder (Duisberg, Germany) at 190°C and 120 rpm for 10 min. Three sets of samples were prepared. The first set, used for the determination of the structure close to the molten state, was solidified in cold water after it was removed from the mixer (quenched samples). The samples used for the determination of structural characteristics and mechanical properties were prepared by the following procedure. The molten material from the chamber was placed into a Fontijne press (Vlaardingen, The Netherlands) preheated to 200°C. After 5 min under a load of 100 kN, the material was transferred from the hot press into a cold press and cooled slowly to laboratory temperature (these were the slowly cooled samples). From the plates obtained, specimens were cut for the tests. The compositions of the prepared blends and their mechanical characteristics are given in Table II. According to SAXS measurements, the quenched and slowly cooled blends of PS–PP 4/1 with the addition of 10% of both BCs differed significantly. These samples were then annealed for 20 min at 190°C and cooled down (these were the annealed samples).

Determination of the tensile impact strength (a_ϵ)

a_ϵ was measured with a Zwick tester (Ulm, Germany) equipped with a special fixture for the test specimen according to DIN Standard 53 448. The maximum pendulum energy was 2 J. All of the measurements were carried out at 23°C. The values obtained are presented as arithmetical means of measurements on 10 specimens.

SAXS

SAXS measurements were performed with a reconstructed Kratky camera with a 60-μm entrance slit and a 42-cm flight path. The used Ni-filtered Cu Kα radiation [wavelength (λ) = 1.54 Å] was recorded with a position-sensitive detector[31] (Joint Institute for Nuclear Research, Dubna, Russia), for which the spatial resolution was approximately 0.1 mm. The intensities were taken in the range of the scattering vector ($\mathbf{q}$) of $(4\pi/\lambda)$ sin Θ from 0.006 to 0.2 Å^{-1} (where 2Θ is the scattering angle). The measured intensities were corrected for constant sample thickness and transmission, primary beam flux, and camera geometry.

SEM

A JSM 6400 (Jeol, Tokyo, Japan) scanning electron microscope was used to study morphology. Samples were fractured in liquid nitrogen and covered with platinum in a Balzers sputter coater (SCD 050) (Lichtenstein).

TEM

Ultrathin sections were prepared to analyze the phase structure of the studied polymers. After the sections were cut at low temperatures with a glass knife of an Ultracut UCT ultramicrotome (Leica, Sollentuna, Sweden), they were stained in osmium tetroxide vapor. For observations and micrographing, TEM (JEM 200 CX, Jeol, Tokyo, Japan) or SEM (Vega, Brno, Czech Republic) with a transmission adapter was used. To diminish the formation of artifacts, we performed sectioning at −130°C. We believe that at this temperature, no substantial changes in sample deformation could occur that would distort the image of the phase structure of the specimens.

RESULTS AND DISCUSSION

SAXS

BCs used as compatibilizers in additive compatibilization are very often organized in an ordered supermolecular structure, manifesting itself by an interference maximum in the region of SAXS.[32,33] Because the compatibilization efficiency of a BC is associated with its interaction with the blend components and, consequently, with the changes of its supermolecular structure, it is convenient to start the study of its structure in compatibilized blends with SAXS. Also, SAXS gives information on a comparatively large sample volume, even if the information concerns the reciprocal space. Microscopic methods show the real structure but from a very small piece of a sample, which can be inhomogeneous. Thus, a combination of scattering and microscopic methods appears to be very useful for investigating a compatibilization process. Moreover, TEM and SEM experiments are relatively time-consuming, whereas the measurement of one SAXS curve takes several minutes. So, we can easily check when a steady state is achieved by comparing the SAXS curves of samples obtained at different preparation

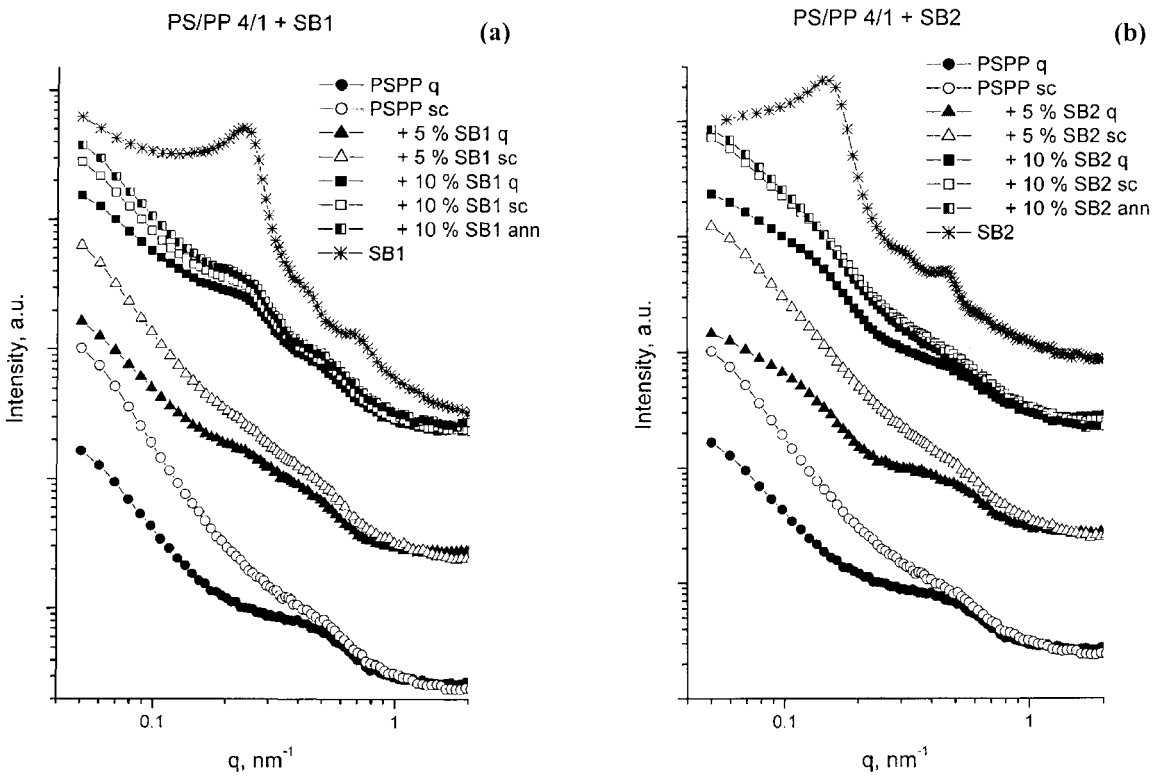

Figure 1 SAXS curves of PS–PP 4/1 blends with the addition of (a) 5 or 10% SB1 and (b) 5 or 10% SB2 (q = quenched; sc = slowly cooled; ann = annealed). The curves are shifted in the *y* axis.

conditions. Then, several chosen samples can be studied by means of electron microscopy methods.

In previous articles, we showed that the appearance of a maximum corresponding to an ordered BC structure on the SAXS curves of compatibilized blends could have different meanings in symmetrical and asymmetrical systems. In PS–PP 4/1 blends with the addition of SB BCs, the interference maximum of a neat BC was observed when a BC with short styrene blocks was added,[22,23] and it was shown by TEM that the ordered BC was a part of the PS–PP interfacial layer. Particles of BCs with long styrene blocks were entrapped in the PS blend component and swollen by the styrene homopolymer or rearranged into micelles to such an extent that the structure of the BC was disordered and no interference maximum was observed.

However, in PS–PB 4/1 blends compatibilized with SB BCs, no maximum corresponding to a neat BC was observed in quenched samples; according to TEM, all of the BCs were dispersed at the PS–PB interface. During slow cooling, the BCs with long styrene blocks maintained their position at the interface, whereas the BCs having short styrene blocks were released from the PS–PB interface, and BC particles with the structure of neat BCs were observed.[28]

A comparison of the structure of quenched and slowly cooled compatibilized samples was now also applied to the structure study of PS–PP blends with varying compositions and compatibilized with SB BCs.

In Figures 1–3, the SAXS curves of PS–PP blends with the addition of 5 or 10 wt % SB1 or SB2 copolymer are shown together with the SAXS curves of the corresponding SB copolymers. The SAXS curves of the compatibilized blends showed two maxima. The maximum at $\mathbf{q} = 0.4\ \mathrm{nm}^{-1}$, corresponding to a long period in semicrystalline PP, was observed also on the SAXS curves of the uncompatibilized samples. The maxima at $\mathbf{q} = 0.24$ and $0.15\ \mathrm{nm}^{-1}$ were attributed to the separated ordered phases of SB1 and SB2, respectively, as they were detected at the same **q** values as the corresponding maxima of the neat SB copolymers.

It was evident that the greatest difference between the quenched and slowly cooled samples was observed for the PS–PP 4/1 blends with the addition of SB2 copolymer [Fig. 1(b)]. We assumed that this BC maintained its supermolecular structure during mixing, but it was partially swollen with styrene homopolymer (see the broad maximum at 0.08–0.15 nm^{-1} in the **q** region on the SAXS curve of the quenched sample). During cooling, the swelling continued, and the maximum of an ordered structure vanished. Also, the presence of SB2 micelles in the PS phase of the blend could not be excluded as both the

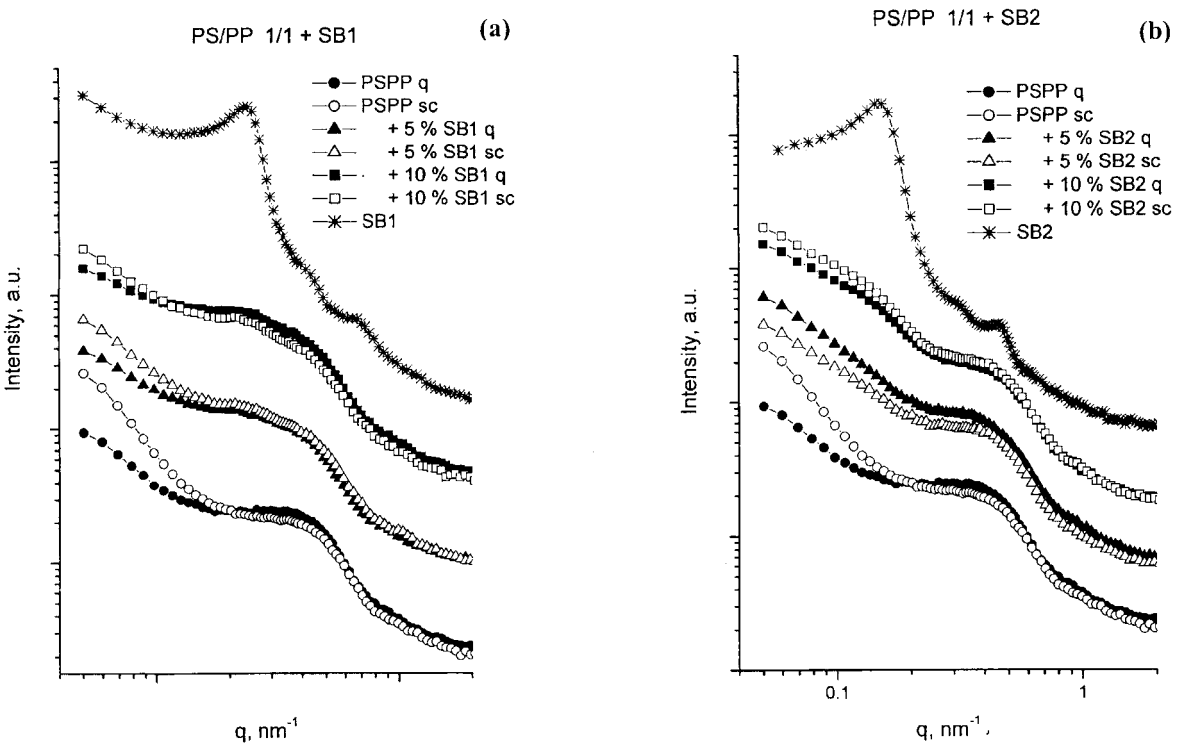

Figure 2 SAXS curves of PS–PP 1/1 blends with addition of (a) 5 or 10% SB1 and (b) 5 or 10% SB2 (**q** = quenched; sc = slowly cooled). The curves are shifted in the *y* axis.

formation of swollen particles of a BC and its micellization were observed by us.[22,28]

The SAXS curves of the quenched and slowly cooled samples of PS–PP 4/1 blends with the addition of SB1 [Fig. 1(a)] also differed. An increase in the intensity for $\mathbf{q} \rightarrow 0$ may have indicated some changes in the dispersion of PP particles, and the increasing intensity in the region of **q** corresponding to the position of the interference maximum of the ordered copolymer structure indicated an increasing amount of the SB1 ordered phase in the sample. In any case, it was evident that the melts of both systems, PS–PP 4/1–SB1 and PS–PP 4/1–SB2, were far from the equilibrium state, so diffractograms of samples additionally annealed at 190°C for 20 min before slow cooling were also taken.

SAXS curves of annealed and slowly cooled compatibilized samples [Fig. 1(a,b)] differed again a little in the innermost part of the scattering curve ($\mathbf{q} \rightarrow 0$) because of some changes in the morphology. No interference maximum corresponding to the formation of an ordered SB2 phase was observed in the annealed PS–PP–SB2 blend, but the maximum of the separated SB1 phase in the annealed sample of the PS–PP–SB1 blend showed another slight increase in comparison with the slowly cooled samples.

When the PS amount in the PS–PP blends decreased, the differences in the SAXS curves of the quenched and slowly cooled samples became less pronounced. The SAXS curves of PS–PP 1/1 and PS–PP 1/4 with the addition of 5 or 10 wt % SB1 [Figs. 2(a) and 3(a)] had very similar shapes with a slight maximum at $\mathbf{q} = 0.24\ \text{nm}^{-1}$, corresponding to the separated SB1 phase.

No regular BC structure was observed in PS–PP 1/1 or PS–PP 1/4 blends with the addition of 5 wt % SB2 [Figs. 2(b) and 3(b)] regardless of the cooling regime. On the SAXS curves of both quenched and slowly cooled samples of PS–PP 1/1 and 1/4 with the addition of 10 wt % SB2, a slight and broad maximum appeared in the same **q** region as in PS–PP 4/1 blends with the addition of the SB2 copolymer. So, interactions of the PS block with PS were expected here, but again we could not decide on the basis of the SAXS data if the SB2 structure was disordered because of swelling with styrene homopolymer or if the formation of SB2 micelles with the PB core in the PS phase of the blends took place.

Electron microscopy and mechanical properties

The morphology of all three uncompatibilized blends was examined on fractured samples by SEM, whereas the morphology of compatibilized blends was studied by scanning electron microscopy in the transmission mode (STEM). Details of the PS–PP interface and internal structure of both SB1 and SB2 copolymers were

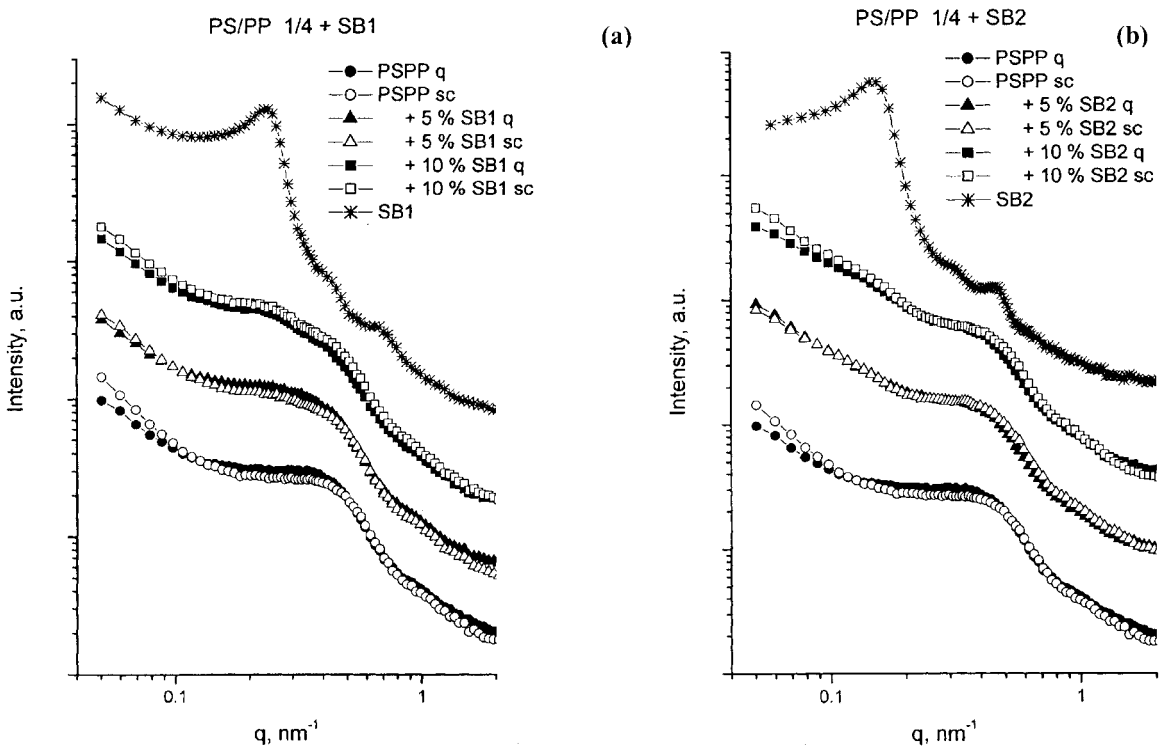

Figure 3 SAXS curves of PS–PP 1/4 blends with addition of (a) 5 or 10% SB1 and (b) 5 or 10% SB2 (**q** = quenched; sc = slowly cooled). The curves are shifted in the *y* axis.

taken with the transmission technique (TEM) at a large magnification.

The aim of this study was to determine both the localization and structure of the selected SB copolymers in the final PS–PP–SB blends with varying PS–PP compositions. As we were not seeking the optimum amount of these BCs necessary for the covering of the PS–PP interface, blends with the addition of 10% SB1 or SB2 were used, where the required effects were pronounced. Because, according to SAXS, the largest differences between quenched and slowly cooled samples were observed with the PS–PP 4/1 blends, these blends were also studied by electron microscopy in more detail than the blends with 50 or 20% PS.

PS–PP 4/1 blends

In Figure 4, the SEM micrographs of quenched and slowly cooled samples of uncompatibilized PS–PP blends are shown. As was expected from the SAXS curves of these samples [see Fig. 1(a)], the morphology of this blend underwent large changes at cooling. During the relaxation, the coalescence of PP particles took place, and huge and anisometric particles appeared.

In Figure 5, micrographs of PS–PP 4/1 blends with the addition of 10% SB1 or SB2 are shown. The mixture of these BCs with the basic blend led in both cases to a much finer dispersion, but the morphologies of PS–PP–SB1 and PS–PP–SB2 differed significantly. In

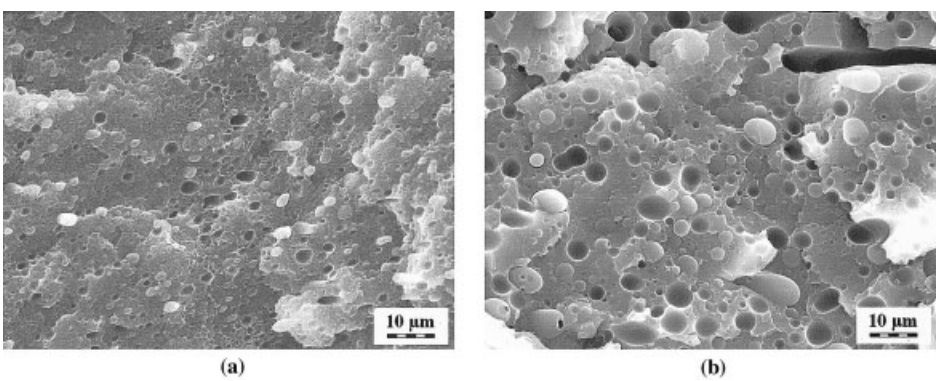

Figure 4 SEM micrographs of uncompatibilized PS–PP 4/1 blends: (a) quenched and (b) slowly cooled samples.

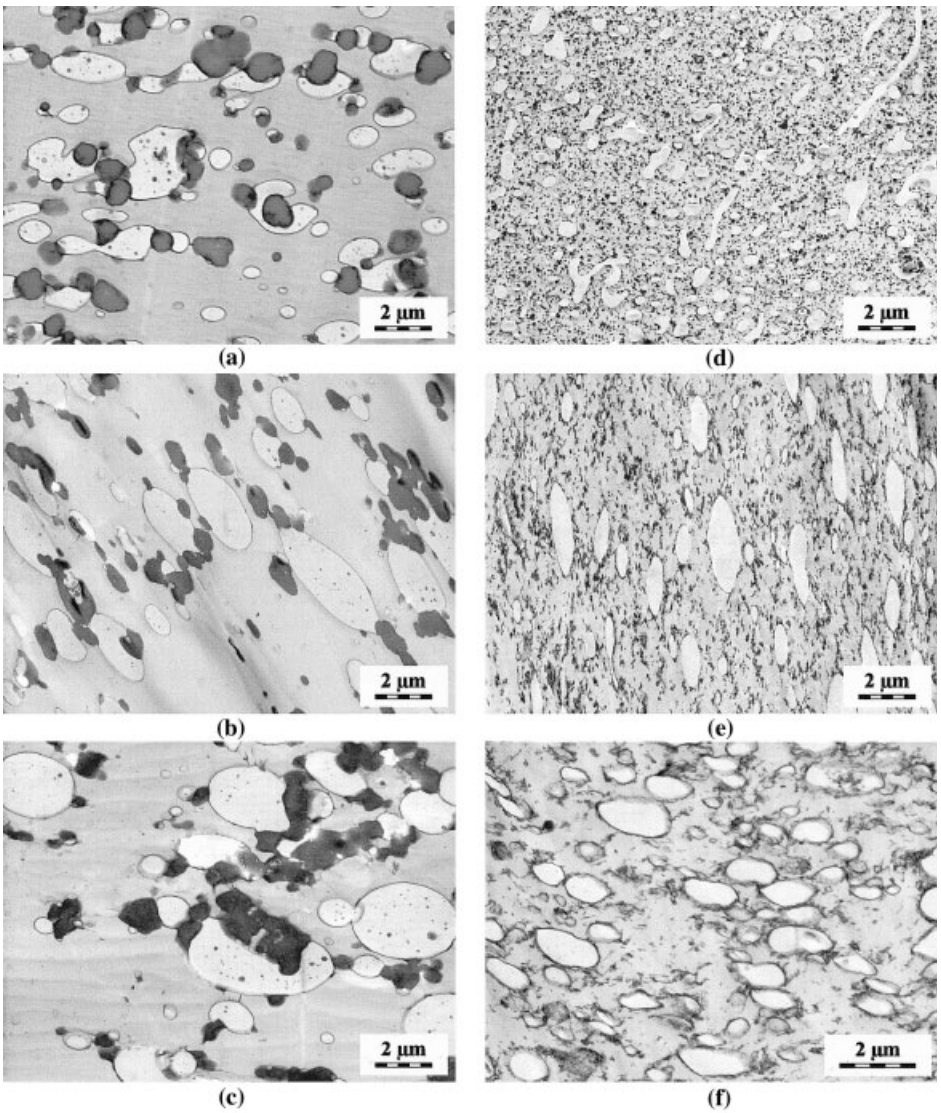

Figure 5 STEM micrographs of PS–PP 4/1 blends with addition of (a) quenched, (b) slowly cooled, and (c) annealed 10% SB1 samples and (d) quenched, (e) slowly cooled, and (f) annealed 10% SB2 samples.

quenched PS–PP–SB1 blends [Fig. 5(a)], PP particles were observed with dimensions of 0.5–5 μm and were covered by a relatively thick BC layer. Besides, the particles of the SB1 copolymer appeared attached to the PP particles, having, according to SAXS, an inner structure of a neat SB1 copolymer. In addition, tiny SB1 particles were observed incorporated in the PP particles. During cooling, the SB1 copolymer probably escaped from the PS–PP interface, as the SB1 enveloped around the PP particles became thinner and coalesced [Fig. 5(b)]. This process was even more pronounced in the annealed samples of PS–PP–SB1 blends [Fig. 5(c)]. Here, the PP particles were much larger than in the quenched blends. The reason for the coalescence of the PP particles was evidently an additional organization of the separated phase of the SB1 copolymer, which was attached to the PP particles as large objects and, hence, caused a worse covering of the interface by the copolymer. The small SB1 particles inside the PP phase were observed in all three types of the samples, regardless of the temperature regime.

However, the PS–PP interface was qualitatively the same in all three types of the blends, quenched, slowly cooled, and annealed, as is shown in Figure 6, where the TEM micrographs at large magnification are presented. Both SB1 copolymer layers around the PP particles and clusters of separated ordered SB1 phase were detected.

In PS–PP–SB2 blends, quite a different morphology was observed from that of PS–PP–SB1, but even more substantial structural changes depending on the temperature regime were also observed. The dispersion of PP particles in quenched samples [Fig. 5(d)] was surprisingly fine, even though practically all of the SB2 copolymer was distributed in the PS phase as very

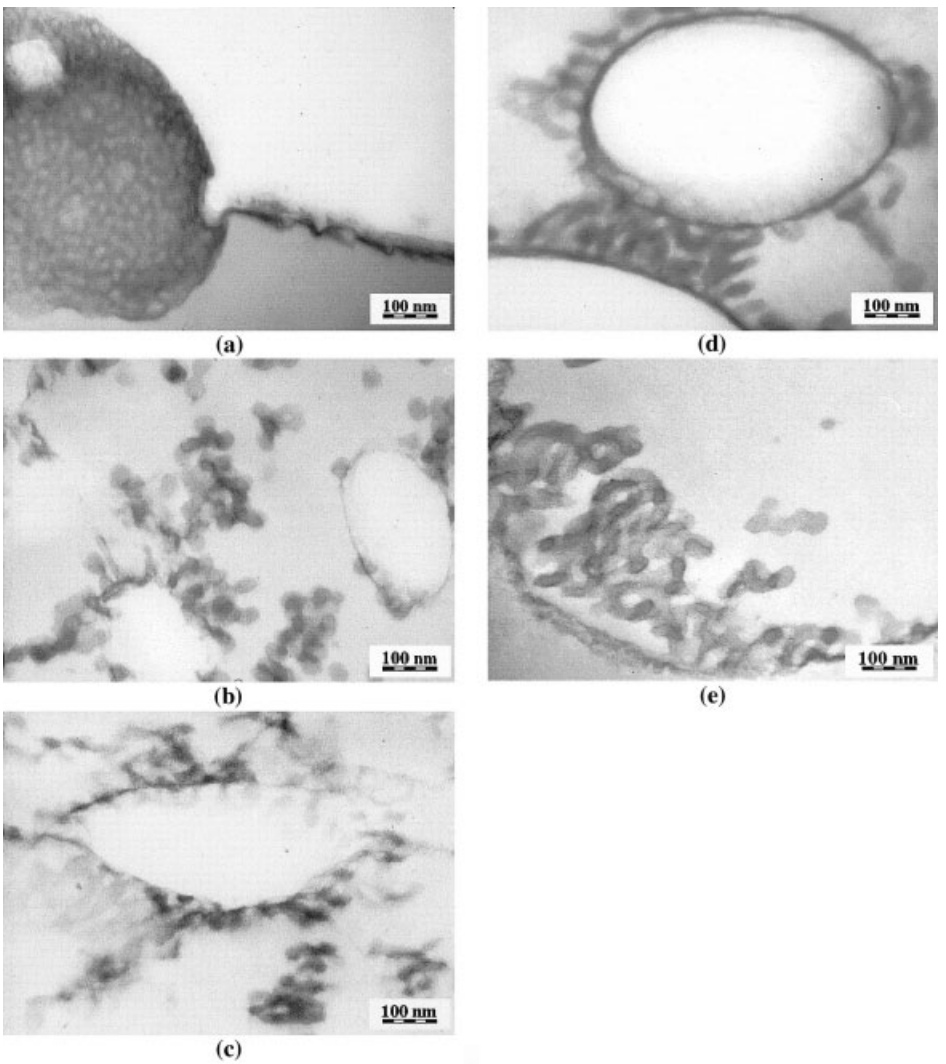

Figure 6 TEM micrographs of the PS–PP interface taken at a large magnification: (a) slowly cooled PS–PP 4/1 + 10% SB1 samples; (b) quenched, (c) slowly cooled, and (d) annealed PS–PP 4/1 + 10% SB2 samples; and (e) slowly cooled PS–PP 1/4 + 10% SB2 samples.

small particles. As the ordered structure of the neat SB2 copolymer was lost, according to SAXS, the swelling of the BC with styrene homopolymer or the formation of SB2 micelles was expected. No SB2 enveloped around the PP particles; also, no spots of SB2 in the PP particles were observed. During cooling, the PP particles became larger; a part of SB2 was localized at the PS–PP interface [Fig. 5(e)]. In annealed samples, this process continued, similar to PS–PP–SB1, but the motion of SB2 in the blend was quite different from that of SB1. SB2 particles (or micelles) in a quiescent molten blend migrated toward the PS–PP interface, and in the end, they formed thick, pronounced envelopes around the PP particles [Fig. 5(f)].

This process is shown in detail in Figure 6(b–d), where the PS–PP–SB2 interface was taken by TEM at a large magnification. In quenched samples [Fig. 6(b)], the PS–PP interface was occupied only randomly by separated SB2 micelles or by their clusters. The formation of these micelles was evidently a result of interactions between the SB2 copolymer and the PS component of the PS–PP blends, as can be deduced from Figure 7, where the TEM micrographs of PS–SB2 are shown. In quenched samples of PS with the addition of 10% SB2, separated micelles of this BC with a PB core and a PS corona were observed, whereas during the slow cooling, the aggregation of these micelles into larger objects took place. In PS–PP–SB2 blends, this aggregation proceeded also but predominantly at the PS–PP interface, and thus, the interfacial layer grew in the slowly cooled samples [Fig. 6(c)]; in the annealed samples, these aggregates formed even bridges between the PP particles [Fig. 6(d)]. The interactions of SB copolymers with long PS blocks with the styrene homopolymer were also confirmed by both SAXS and TEM in our previous studies,[21,22] but it was shown in those studies that no such interactions of these BCs took place in PP.

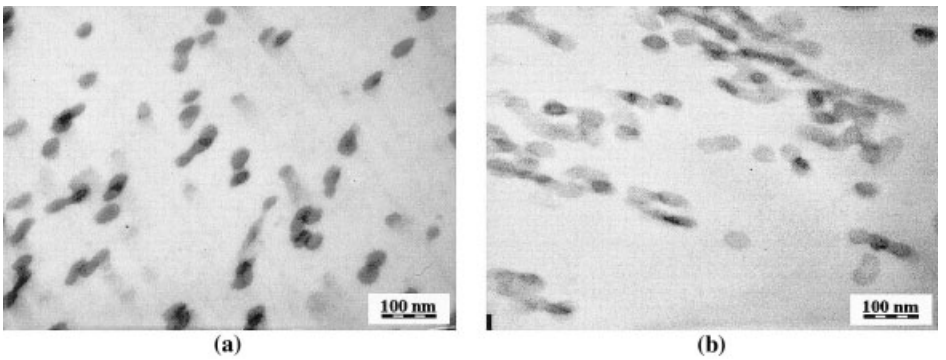

Figure 7 TEM micrographs of PS with addition of 10% SB2: (a) quenched and (b) slowly cooled samples.

Thus, the broad maximum on the SAXS curves of the quenched samples of PS–PP–SB2 blends in the region of small **q** values could be attributed to the scattering curve of the SB2 micelles. On the SAXS curves of the slowly cooled and annealed samples of these blends, a strong increase in the intensity was observed for $\mathbf{q} \rightarrow 0$ because of changes in the morphology that may have led to an overlap of this curve.

The results of SAXS and electron microscopy were also supported by the measurement of a_ϵ in these samples (Table II). The addition of both SB1 and SB2 copolymers to the PS–PP 4/1 blend led to a remarkable increase in the values of a_ϵ in comparison with those of the uncompatibilized blend, but there were differences between slowly cooled and annealed samples in PS–PP–SB1 and PS–PP–SB2 blends. Although in annealed PS–PP–SB1 samples, the value of a_ϵ (20.6 kJ/m^2) decreased in comparison with the slowly cooled ones (a_ϵ = 29.0 kJ/m^2), because of the escape of SB1 from the PS–PP interface in annealed samples of PS–PP–SB2, the value of a_ϵ increased to 44.9 kJ/m^2 compared with the a_ϵ value 30.0 kJ/m^2 found in the slowly cooled samples. This increase was, of course, caused by the enrichment of the PS–PP interfacial layer in SB2 and by a subsequent increase in the interphase adhesion. These results were also in a good agreement with the SAXS experiments.

These results clearly demonstrate that the distributions of SB1 and SB2 copolymers between the interface and bulk phase in the PS–PP 4/1 blends strongly differed for steady mixing and for the quiescent state. It turns out that common predictions of the ability of BCs to cover the interface, based on the rules of equilibrium thermodynamics, have only limited applicability to prediction of the morphology and properties of compatibilized polymer blends. The coalescence of PP particles in a molten quiescent PS–PP–SB1 blend was in agreement with the results of Maric and Macosko,[34] who found that short BCs show a strong emulgation effect in mixing but they do not prevent coalescence in the quiescent blend. The strong improvement in the covering of the PS–PP interface by SB2 after annealing (annealed samples) and a substantial increase in a_ϵ of the annealed PS–PP–SB2 blends were somewhat surprising; we did not find a similar effect in the literature. These results led us to the practically important conclusion that the compatibilization efficiency of SB BCs generally depends on the conditions of the blend preparation and processing.

PS–PP 1/1 and 1/4 blends

According to the SAXS measurements, the quenched and slowly cooled samples of both PS–PP 1/1 and PS–PP 1/4 blends did not differ significantly from each other, so we assumed that another temperature relaxation did not significantly affect the structure of simply pressed (slowly cooled) samples. Thus, in Figure 8, the only micrographs given are of the slowly cooled samples of basic PS–PP blends with the addition of 10% SB1 or SB2.

In the PS–PP 1/1 uncompatibilized blend, a morphology very close to a cocontinuous structure was observed [Fig. 8(a)]. The addition of 10% SB1 led to a change in the type of structure, and the formation of PS particles took place [Fig. 8(b)], even if the structure was very coarse and practically no SB1 envelopes around the PS particles were observed. The change in the type of the phase structure at a certain blend composition by the addition of a compatibilizer has been detected for several systems.[19,35,36] Unfortunately, a plausible theory of this effect has not been available so far. Particles of SB1, having, according to SAXS, the structure of the neat copolymer, were attached to the PS particles, and similar to the PS–PP 4/1–10% SB1 blends, tiny SB1 particles without an ordered structure were observed in the PP phase.

The addition of 10% SB2 to the PS–PP 1/1 blend influenced the morphology of the basic blend less remarkably [Fig. 8(c)]. Particles of PS were also observed here, but they were enormously elongated, so the structure reminded us more of the cocontinuous than of the particle morphology. The SB2 copolymer was completely dispersed in the PS particles, and

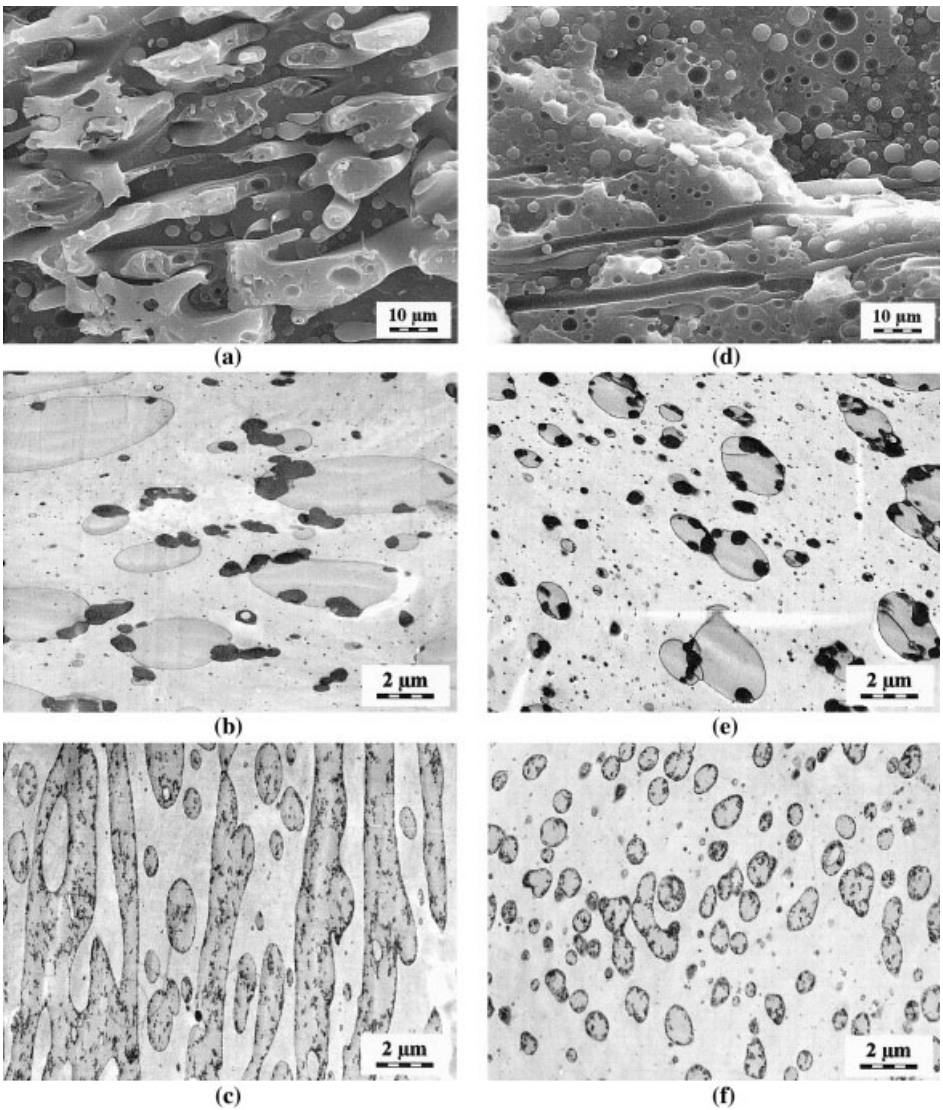

Figure 8 STEM micrographs of PS–PP 1/1 slowly cooled blends: (a) uncompatibilized, (b) with the addition of 10% SB1, and (c) with the addition of 10% SB2. STEM micrographs of slowly cooled PS–PP 1/4 blends: (e) uncompatibilized, (f) with the addition of 10% SB1, and (g) with the addition of 10% SB2.

according to SAXS, its ordered supermolecular structure was lost.

An increase in the value of a_ϵ in the PS–PP–SB1 blend compared with the basic PS–PP 1/1 blend from a_ϵ = 32.6 to 41.5 kJ/m^2 was attributed to the change in the morphology or it may have been caused by the presence of an elastomeric SB1. A remarkably higher increase in a_ϵ in the PS–PP–SB2 blend up to a value of 55.0 kJ/m^2 could be explained by the preferential localization of the SB2 particles dispersed in the PS phase near to the PS–PP interface.

The morphology of the uncompatibilized PS–PP 1/4 blend was similar to that observed in the PS–PP 4/1 sample with the reverse ratio of the dispersed phase and matrix. Here also, two types of particles, spherical with dimensions of 1–5 μm and strongly elongated ones, were found [Fig. 8(d)]. Also, the structure of this blend compatibilized with 10% SB1 was close to the structure of the corresponding blend with the PS matrix [Fig. 8(e)]. Envelopes of the SB1 copolymer around PS particles were well developed, and SB1 particles, having, according to SAXS, the structure of the neat copolymer, were attached to the PS–PP interface. Tiny SB1 particles dispersed in the PP phase were also observed here. Also, the dimensions of the dispersed particle (PP or PS) were not very different. As a similar morphology was found in both these blends, approximately the same increase in a_ϵ in PS–PP–SB1 blends and PS–PP was not surprising (see Table II).

In PS–PP 1/4 blends with the addition of 10% SB2, a very fine morphology was observed. The SB2 copolymer was mostly dispersed in PS particles with average dimensions of 1–2 μm. Clusters of SB2 micelles, similar to those observed in annealed samples of the

PS–PP 4/1 blend with the addition of 10% SB2, were preferably localized at the PS–PP interface [Fig. 6(e)].

The formation of this layer at the PS–PP interface rich in SB2 led to a remarkable increase in a_ϵ in these blends, similar to that observed in the annealed PS–PP–SB2 samples with the PS matrix. Somewhat surprising was a strong difference between the a_ϵ of the blends compatibilized with 5 and 10% SB2, that is, with 25 and 50% compatibilizer relative to the dispersed phase. Normally, it is assumed that saturation of the interface appears well below 20% compatibilizer relative to the dispersed phase.[8] In our opinion, neither SB2 subinclusions into the PS particle nor small SB2 particles in the PP matrix should have had a pronounced effect on the impact strength (SB2 contained more than 50% PS).

CONCLUSIONS

The localization of a SB triblock copolymer in PS–PP blends and its structure modification depended to a large extent on the length of its styrene blocks. SB1 copolymer, having short styrene blocks (MW $<$ 18,000), maintained the ordered supermolecular structure of the neat copolymer, and its particles were attached to the PS–PP interface, regardless of the blend composition. Also, in PS–PP 4/1 and PS–PP 1/4 blends, where a pronounced particle structure was observed, this copolymer also became a part of the PS–PP interfacial layer, thus improving the interfacial tension. The SB2 triblock copolymer, with styrene blocks long enough to form entanglements with the styrene homopolymer, was entrapped in the PS phase of the resulting blends as micelles. In blends with high contents of SB2 relative to PS, SB2 covered the interface. In blends with the PS matrix, this phenomenon was observed only after sufficiently long temperature relaxation. The addition of SB1 changed the type of the phase structure of the PS–PP 1/1 blend. Despite differences in the location and structure of BCs, the related PS–PP 4/1 blends compatibilized with SB1 and SB2 showed practically the same increase in the impact strength when compared with uncompatibilized blends. The same was true for PS–PP 1/4 with 5% BCs. The addition of SB2 led to a greater improvement in the impact strength than that of SB1 in PS–PP 1/1 blends and PS–PP 1/4 blends with 10% BC.

A pronounced migration of SB2 to the interface was found in the molten quiescent PS–PP 4/1 blend. However, coalescence and a worsening of the interface coverage were observed in PS–PP 4/1 blends with SB1. These changes in the structure were strongly reflected by the impact strength. The described effects clearly showed that the location of SB1 and SB2 copolymers in thermodynamic equilibrium and in the steady state differed substantially, depending on intensive mixing. Generally, the compatibilization efficiency of SB copolymers in PS–PP blends depended on the conditions of blend mixing and processing and could not be predicted with the rules of equilibrium thermodynamics only.

References

1. Utracki, L. A. Polymer Alloys and Blends; Hanser: Munich, 1989.
2. Sjoerdsma, S. D.; Bleijenberg, A. C. A. M.; Heikens, D. Polymer 1981, 22, 619.
3. Fayt, R.; Jérome, R.; Teyssié, P. J Polym Sci Part B: Polym Phys 1989, 27, 775.
4. Brahimi, B.; Ait-Kadi, A.; Ajji, A.; Fayt, R. J Polym Sci Part B: Polym Phys 1991, 29, 945.
5. Xu, G.; Lim, S. Polymer 1996, 37, 421.
6. Taha, M.; Frerejean, V. J Appl Polym Sci 1996, 61, 969.
7. Wagner, M.; Wolf, B. A. Polymer 1993, 34, 1460.
8. Cigana, P.; Favis, B. D.; Albert, C.; Vu-Khanh, T. Macromolecules 1997, 30, 4163.
9. Appleby, T.; Czer, F.; Moad, G.; Riyyardo, E.; Stavropoulos, C. Polym Bull 1994, 32, 479.
10. Kroeze, E.; ten Brinke, G.; Hadziioannou, G. Polym Bull 1997, 38, 210.
11. Del Quidice, L.; Cohen, R. E.; Attalla, G.; Bertinotti, F. J Appl Polym Sci 1985, 30, 4305.
12. Tjong, S. C.; Xu, S. A. J Appl Polym Sci 1998, 68, 1099.
13. Radonjič, G.; Musil, V.; Šmit, I. J Appl Polym Sci 1998, 69, 2625.
14. Radonjič, G.; Musil, V. Angew Makromol Chem 1997, 251, 141.
15. Hermes, H.; Higgins, J. S. Polym Eng Sci 1998, 38, 8477.
16. Barlow, J. W.; Paul, D. R. Polym Eng Sci 1984, 24, 525.
17. Hong, B. K.; Jo, W. H. Polymer 2000, 41, 2069.
18. Harrats, C.; Fayt, R.; Jérome, R. Polymer 2002, 43, 863.
19. Fortelný, I.; Michálková, D.; Hromádková, J.; Lednický, F. J Appl Polym Sci 2001, 81, 570.
20. Horák, Z.; Fořt, V.; Hlavatá, D.; Lednický, F.; Večerka, F. Polymer 1996, 37, 65.
21. Hlavatá, D.; Horák, Z.; Hromádková, J.; Lednický, F. Polym Networks Blends 1997, 7, 195.
22. Hlavatá, D.; Horák, Z.; Hromádková, J.; Lednický, F.; Pleska, A. J Polym Sci Part B: Polym Phys 1999, 37, 1647.
23. Hlavatá, D.; Horák, Z.; Hromádková, J.; Lednický, F.; Pleska, A.; Zanevsky, Y. J Polym Sci Part B: Polym Phys 2001, 39, 931.
24. Horák, Z.; Hlavatá, D.; Fortelný, I.; Lednický, F. Polym Eng Sci 2002, 42, 2042.
25. Wu, S. Polym Eng Sci 1990, 30, 753.
26. Kavassalis, T. A.; Noolandi, J. Macromolecules 1989, 22, 2709.
27. Fortelný, I.; Hlavatá, D.; Michálková, D.; Mikešová, J.; Potroková, L.; Šloufová, I. J Polym Sci Part B: Polym Phys 2003, 41, 609.
28. Horák, Z.; Hlavatá, D.; Hromádková, J.; Kotek, J.; Hašová, V.; Mikešová, J.; Pleska, A. J Polym Sci Part B: Polym Phys 2002, 40, 2612.
29. Čermák, J., Hašová, V.; Mačka, M.; Petrů, V.; Pleska, A.; Reiss, J.; Sufčák, M.; Večerka, F.; Vyoral, L. Czech Pat. 254,630 (1988); Chem Abstr 1989, 111, 59375.
30. Pulda, J. Collect Pap Rubber Plast Res 1997, 4, 109 (in Czech).
31. Chernenko, S. P.; Cheremukhina, G. A.; Fateev, O. V.; Smykov, L. P.; Vasiliev, S. E.; Zanevsky, Y. V.; Kheiker, D. M.; Popov, A. N. Nucl Instrum Methods Phys Res Sect A 1994, 348, 261.
32. Sadron, C.; Galott, B. Makromol Chem 1973, 164, 301.
33. Bates, F. S.; Cohen R. E.; Berney, C. V. Macromolecules 1982, 15, 589.
34. Maric, M.; Macosko, C. W. J Polym Sci Part B: Polym Phys 2002, 40, 346.
35. Navrátilová, E.; Fortelný, I. Polym Networks Blends 1996, 6, 127.
36. Lyngaae-Jørgensen, J.; Lunde Rasmussen, K.; Chtcherbakova, E. A.; Utracki, L. A. Polym Eng Sci 1999, 39, 1060.